Tumor and Stem Cell Biology

Cancer Research

ADAMTS1 Contributes to the Acquisition of an Endothelial-like Phenotype in Plastic Tumor Cells

Carmen Casal[1], Antoni Xavier Torres-Collado[2], María del Carmen Plaza-Calonge[1], Estefanía Martino-Echarri[1], Santiago Ramón y Cajal[3], Federico Rojo[4], Arjan W. Griffioen[5], and Juan Carlos Rodríguez-Manzaneque[1]

Abstract

Cancer stem cells have been hypothesized to explain tumor plasticity, including the capability to adopt distinct differentiation commitments. Among the mechanisms of tumor neovascularization, the ability of some malignant cells to mimic an endothelial phenotype has been recognized by a capacity to form matrix-enriched pseudovascular structures. In addition to the expression of genes associated with an endothelial nature, the molecular dynamism of specific microenvironments may also be critical. Here, we report the identification of the extracellular protease ADAMTS1 as a critical molecule for tumor cells to acquire endothelial-like properties. In a fibrosarcoma model, ADAMTS1 increased tumor growth rate in an angiogenesis-independent manner, influencing the tumor cells to display an exclusive endothelial-like gene signature. We documented the relevant expression of ADAMTS1 in aggressive and highly plastic melanoma and Ewing sarcoma cells. Notably, inhibiting ADAMTS1 action compromised the endothelial mimetic attributes observed in this setting. Our findings provide insights into how the tumor microenvironment can elicit endothelial mimicry by tumor cells.
Cancer Res; 70(11); 4676–86. ©2010 AACR.

Introduction

Events of tumor neovascularization are a basic principle during tumor progression. Although the process of angiogenesis has been recognized as the major protagonist, alternative mechanisms have been highlighted in literature (1). Among these specialized mechanisms is the plasticity of some tumor cells to acquire endothelial-like (EL) properties to align and form pseudovascular structures (2). This phenomenon was first described in aggressive melanomas and is called vasculogenic mimicry (VM; ref. 3), due to genotypic and phenotypic characteristics that are reminiscent of embryonic vasculogenesis. Another example of tumor plasticity is the process of cellular differentiation from cancer stem cells (CSC). Thus far, most of the research about CSCs hypothesizes that these cells possess proliferative and self-renewal potential that is necessary to generate a new emerging tumor. Like normal tissue stem cells, CSCs are expected to display a range of differentiation capabilities, a feature that has not been deeply studied. Importantly, research with various types of sarcoma tumors has revealed their mesenchymal-like differentiation properties. For example, the origin of Ewing sarcomas, the second most frequent bone tumor in young people, has provoked an interesting debate. First named as "endothelioma" of the bone by James Ewing (4), DNA microarray studies later confirmed their endothelial and neural crest-derived origin (5). Indeed, published reports underlined the mesenchymal stem cell features in Ewing tumors and in other bone and soft tissue cancers (6–8).

The role of the microenvironment for tumor plasticity has been studied under various conditions. First, the importance of mechanical and physical properties of the matrix has been reported to play a main role in stem cell commitment (9) and tumorigenesis (10). Second, emerging studies have shown that aggressive tumor cells can be reprogrammed in embryonic microenvironments (11). As for the stem cell niche, its characterization has been limited to cellular components (12) although the role of extracellular factors, including proteases, requires further attention.

ADAMTS1 represents the first described member of the ADAMTS (a disintegrin and metalloproteinase with thrombospondin motifs) family of proteases (13). It has been reported to display antiangiogenic properties (14, 15); however, its mechanism of action during tumor progression seems controversial. Protumorigenic and prometastatic roles of ADAMTS1 have been proposed by induction of a

Authors' Affiliations: [1]GENYO (Pfizer-University of Granada-Andalusian Government Centre for Genomics and Oncological Research), Armilla, Granada, Spain; [2]Medical Oncology Research Program and [3]Department of Pathology, Vall d'Hebron University Hospital Research Institute; and [4]Oncology Service, Hospital del Mar-IMIM, Barcelona, Spain; and [5]Department of Medical Oncology, VU University Medical Center, Amsterdam, the Netherlands

Note: Supplementary data for this article are available at Cancer Research Online (http://cancerres.aacrjournals.org/).

C. Casal and A.X. Torres-Collado contributed equally to this work.

Corresponding Author: Juan Carlos Rodríguez-Manzaneque, GENYO-Centro de Investigación Biomédica, Armilla 18100, Granada, Spain. Phone: 349-582-41000, ext. 20360; Fax: 349-588-19132; E-mail: juancarlos.rodriguez@genyo.es.

doi: 10.1158/0008-5472.CAN-09-4197

stromal reaction (16) and by its activity on epidermal growth factor–like ligands (17, 18).

Here, we report that the overexpression of ADAMTS1 in a fibrosarcoma model caused an increased tumor growth rate that is angiogenesis independent. A closer analysis showed a relevant staining of periodic acid-Schiff (PAS)/laminin 5γ2–positive loops and an exclusive EL gene signature in tumor cells. We further observed the presence of ADAMTS1 protease in aggressive melanoma and Ewing sarcoma cells, previously characterized by their capacity to mimic vasculogenic-related events. Our studies showed both mesenchymal and EL commitments of Ewing tumor cells. Finally, the inhibition of ADAMTS1 compromised their endothelial mimesis.

Materials and Methods

Cell culture

Human Ewing sarcoma (EW7, SIM/EW27, and RD-ES) and human melanoma (MUM2B, MUM2C, C8161, and C81-61) cell lines (provided by Dr. Griffioen, VU University Medical Center, Amsterdam, the Netherlands) were cultured in RPMI with 10% fetal bovine serum (FBS), 5 mmol/L L-glutamine, and 1% penicillin-streptomycin. Human fibrosarcoma HT1080 cells (from the American Type Culture Collection) were cultured in DMEM with 10% FBS, 5 mmol/L L-glutamine, and 1% penicillin-streptomycin. All cells were maintained at 37°C, 5% CO_2. Full-length human ADAMTS1 used for stable clones was described elsewhere (19). If required, conditioned medium was concentrated with Strataclean Resin (Stratagene). Cell layer was harvested with radioimmunoprecipitation assay buffer [20 mmol/L Tris-HCl (pH 8), 150 mmol/L NaCl, 0.1% SDS, 1% NP40, 1 mmol/L EDTA]. For capillary-like formation assays, 25 μL of Matrigel (BD Biosciences) were spread onto eight-chamber BD Falcon glass culture slides (BD Biosciences) or onto 96-well plate. Cells were seeded at 2.5×10^4 cells per well (high density) in eight-chamber slides and at 5×10^3 cells per well (low density) in 96-well plates, and maintained with RPMI-1% FBS. Tissue inhibitor of metalloproteinase (TIMP) treatments were performed with 1 μmol/L TIMP1 or TIMP3 (R&D Systems) added to Matrigel before polymerization. For cocultures, either human umbilical vascular endothelial cell (HUVEC) or EW7 cells were labeled with 20 μg/mL of Cell Tracker CM-Dil (C7000, Molecular Probes). HUVEC (1.5×10^4) were cocultured with 1.0×10^4 EW7 cells in an eight-chamber culture slide coated with Matrigel. After 24 hours, cells were fixed with 4% formaldehyde and stained with 4′,6-diamidino-2-phenylindole (DAPI). Images were captured with an Axiocam MRM digital camera (Zeiss) attached to an AxioImager A1 microscope (Zeiss). For adipogenic and osteogenic differentiation, 1.5×10^5 EW7 cells were seeded in a 12-well plate and incubated with media from StemPro Adipogenesis and Osteogenesis differentiation kits as indicated (Life Technologies Invitrogen). Finally, cells were stained with Oil Red O (Sigma) to visualize lipid vesicles or with 2% Alizarin Red solution (Sigma) to visualize calcium deposits.

In vitro three-dimensional tubulogenesis fibrin gel bead assay

The fibrin gel bead assay was adapted from the described for endothelial cells (20). Here, EW7 sarcoma cells were allowed to attach to Cytodex-3 microcarrier beads (GE Healthcare) by incubation in complete medium for 4 hours at 37°C (1×10^6/2,500 beads). Coated beads were suspended in a larger volume of medium and incubated under agitation for 3 days. Finally, beads were embedded in a fibrin matrix (50 beads/mL). Pictures were captured at the indicated times with ×5 and ×20 objectives using an Axiocam ICC3 digital camera (Zeiss) attached to an Axiovert 40CFL microscope (Zeiss).

Generation of ADAMTS1-knockdown cells

Stable shRNA (short hairpin RNA)–mediated knockdown clones were achieved with MISSION vectors (Sigma). Briefly, 293T cells were cotransfected (with FuGENE 6) with lentivirus envelope and gag-pol elements (provided by Dr. Recio, Vall d'Hebron University Hospital Research Institute, Barcelona, Spain) in addition to lentiviral MISSION shADAMTS1 or MISSION nontarget shRNA control vectors. Viruses were used to infect target cells in the presence of 8 μg/mL polybrene. Different shADAMTS1 clones were selected with 0.5 μg/mL puromycin.

Tumor xenograft assays

Nu/Nu BALB/c mice (5 per group) were s.c. injected in the right flank with 5×10^6 cells per 200 μL. Mice weight and tumor size were assessed every 3 days after cell injection. Tumor volumes were calculated by the equation $D^*d^{2*}\pi/6$ in which D is the tumor diameter at its widest and d at its smallest (21). Test subjects were sacrificed after 21 days following proper guidelines.

Immunoblot analysis

Samples were subjected to SDS-PAGE and transferred to nitrocellulose and polyvinylidene difluoride membranes. After blocking with 5% low-fat milk, membranes were incubated with the monoclonal antibody mouse anti-human ADAMTS1 [clones 5D4E11B5 and 3E46B4 (provided by Dr. Iruela-Arispe, University of California, Los Angeles, Los Angeles, CA)]. Signal was detected with the SuperSignal WestDura kit (Pierce).

Immunohistochemistry

Antigen retrieval was approached in two different ways: (*a*) Proteinase K: 20 minutes at 37°C, for VE-cadherin and laminin 5γ2 antibodies, and (*b*) Tris-EDTA (10 mmol/L Tris, 1 mmol/L EDTA; pH 8): 10 minutes at 650 Watt microwave followed by 10 minutes at room temperature for CD31 antibodies. Later, sections were blocked and incubated with the following primary antibodies: polyclonal rat anti-mouse CD31 (9F1; 1:10 dilution), monoclonal mouse anti-human laminin 5γ2 (1:100 dilution; Novocastra), polyclonal rabbit anti–FVIII-related antigen (Chemicon), polyclonal rabbit anti-human VE-cadherin (1:100 dilution; Cayman Laboratories), and monoclonal mouse anti-human ADAMTS1 (clone 3E46B4). Final visualization was obtained with the Envision

system (DAKO). PAS staining (Sigma) was done following standardized methods. Microvessel density was determined by the Chalkley morphometry analysis (immunostaining with anti–FVIII-related antigen antibody). For frozen tissue sections, visualization was obtained by incubation with 3,3′-diaminobenzidine. For phalloidin staining, Phalloidin-Texas red was added to fixed and permeabilized cells for 45 minutes and slides were mounted with the Vectashield mounting media with DAPI (Vector).

RNA isolation and reverse transcription-PCR analysis

Total RNA was isolated from cells and tissue sections using the NucleoSpin RNA II kit (Macherey-Nagel) followed by RNase-free DNase treatment (Macherey-Nagel). cDNA synthesis was done with 1 μg of total RNA using the iScript cDNA synthesis kit (Bio-Rad). Reverse transcription-PCR (RT-PCR) was performed using EcoTaq DNA polymerase (Byoline) with the specific primers (Supplementary Table S1). Quantitative RT-PCR (qRT-PCR) was done using the Power SYBR Green PCR Master Mix (Applied Biosystems) using 7500 Real-time PCR System with the specific primers (Supplementary Table S2). The expression of each target gene was normalized to the expression of glyceraldehyde-3-phosphate dehydrogenase or β-actin.

Results

Effects of ADAMTS1 expression in an HT1080 fibrosarcoma model and analysis of neovascularization and related features

To study the role of this protease during tumor progression, HT1080 fibrosarcoma cells were modified to overexpress ADAMTS1 protein (Fig. 1A). The s.c. injection of modified and control cells in nude mice induced the development of a tumor mass, which was monitored over a period of 21 days. Although initial growth rate was similar for both cases, significant differences were detected at day 10 and at day 21, when the animals were sacrificed. Mice injected with ADAMTS1-HT1080 cells developed significantly larger tumors (final volume, fv = 2.65 ± 1.36 cm^3) compared with tumors produced by control cells (fv = 1.31 ± 0.44 cm^3; Fig. 1B), differences that were corroborated by the final tumor mass (Fig. 1C).

Detailed histologic and immunohistochemical evaluation of these tumor specimens was approached to observe any changes in blood vessel development. The initial detection of mouse vessels was achieved by staining with the endothelial-specific markers anti–FVIII-related antigen (Fig. 1D) and anti-mouse CD31 (Fig. 2A, a–b). The results showed relevant changes between the two groups. Contrast to the final tumor mass, the density of mouse vessels decreased in ADAMTS1 overexpressors compared with control xenografts (Fig. 1D). In an attempt to reconcile the differences between tumor growth and vessel density, the relevance of alternative mechanisms of neovascularization was evaluated. PAS staining, a known method used in various tumor models, was performed to identify vascular and pseudovascular networks (3). Although positive PAS staining was visualized in all cases, networks resembling the described VM structures were mainly detected in tumors derived from ADAMTS1-overexpressing cells (Fig. 2A, c–d). Because this staining procedure does not provide specific molecular information, immunostaining of the tumors with human laminin 5γ2 and VE-cadherin antibodies was performed; these are proteins reported to be overexpressed and important in VM events (22). The laminin 5γ2 pattern observed in the tumors derived from ADAMTS1-overexpressing cells was similar to that observed by PAS staining (Fig. 2A, e–f). VE-cadherin was also present in ADAMTS1-overexpressing tumors

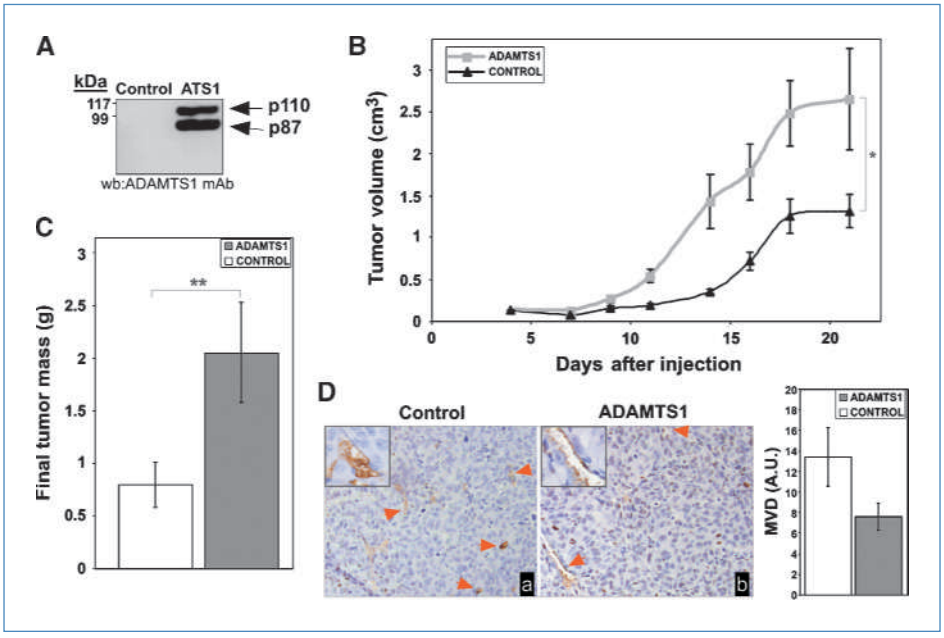

Figure 1. Growth of HT1080 fibrosarcoma tumor xenografts. A, 48-h conditioned medium from a six-well plate (control and ADAMTS1-overexpressing HT1080 cells) was analyzed by Western blot. mAb, monoclonal antibody. B, progression of tumors in HT1080 xenografts. Tumor volume was measured every 3 d until sacrifice. C, representation of final tumor weight of HT1080 xenografts. D, inmunolocalization of mouse blood vessels using anti–FVIII-related antigen antibody in control (Da) and ADAMTS1-overexpressing (Db) HT1080 xenografts. Arrows, positive signals. Inset, a magnification representing a single vascular structure. Graph represents microvessel density (MVD) assayed by the Chalkley method. (*, $P < 0.1$; **, $P < 0.05$, Mann-Whitney U test). A.U., arbitrary units.

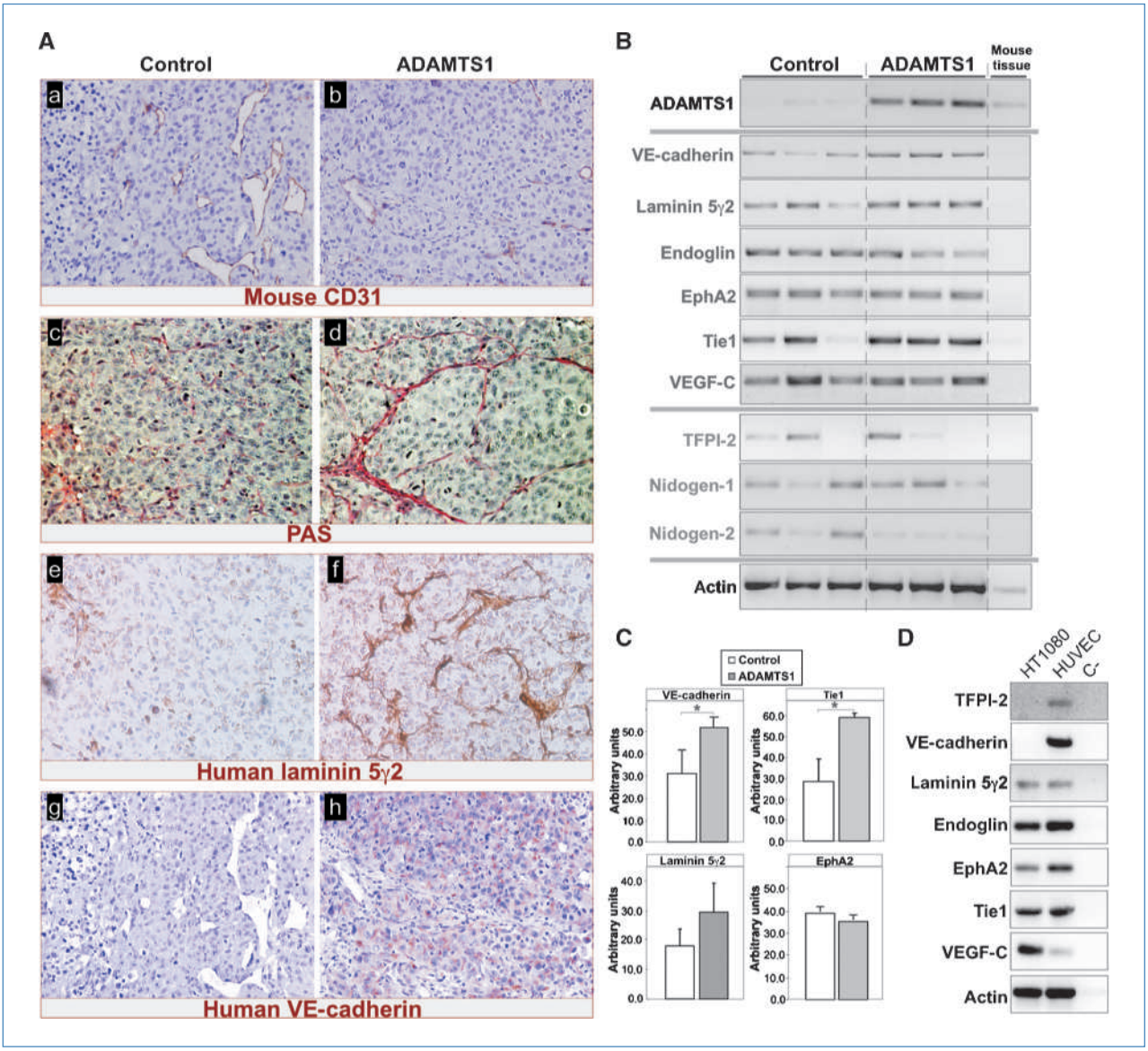

Figure 2. Evidence of an EL phenotype in ADAMTS1-overexpresing HT1080 xenografts. A, a to h, immunodetection in paraffin sections of control (a, c, e, and g) and ADAMTS1-overexpressing (b, d, f, and h) tumors, as follows: a and b, anti-mouse CD31 antibody; c and d, PAS staining; e and f, anti-human laminin 5γ2; and g and h, anti-human VE-cadherin. B, total RNA (0.5 μg) from xenograft samples was subjected to RT-PCR with specific oligos for the human sequences of the indicated genes. Mouse tissue was used as a control for specificity. C, densitometric quantification of *VE-cadherin, laminin 5γ2, Tie1,* and *EphA2* expression normalized versus actin levels in control and ADAMTS1 xenografts (*, $P < 0.1$, Mann-Whitney *U* test). D, gene signature of HT1080 cells compared with HUVEC. Total RNA (0.5 μg) was subjected to RT-PCR with specific oligos for the human genes mentioned above.

whereas its expression was practically absent in control samples (Fig. 2A, g–h).

The expression of various genes implicated in the VM phenomenon and ADAMTS1 substrates TFPI-2 and nidogens 1 and 2 was evaluated by RT-PCR. Importantly, all the designed oligonucleotides were specific for human sequences; thus, detected levels will originate from the grafted human cells. Levels of the endothelial-specific genes *VE-cadherin, Tie1*, and *laminin 5γ2* were upregulated in ADAMTS1-overexpressing tumors (Fig. 2B and C), supporting our previous results from the staining procedures (Fig. 2A). Surprisingly, the expression of these endothelial-specific genes was also detected in control tumors (Fig. 2B). To determine the source of this gene expression, we evaluated control HT1080 cells and compared them with endothelial cells (Fig. 2D). With the exception of *VE-cadherin,* RNA levels of all these molecules were detected in HT1080 parental cells, suggesting that this sarcoma-derived cell line already possessed the potential to be driven into an EL lineage. This property was acquired when cells were implanted into the animals in the presence of the protease ADAMTS1.

With regards to the phenomenon of tumor plasticity and the acquisition of an EL phenotype, we decided to analyze several melanoma and sarcoma cellular models that have been already described as positive for these events (2).

Presence of ADAMTS1 in sarcoma and melanoma cells

We explored the presence of ADAMTS1 in several melanoma and Ewing sarcoma cell lines that have already been classified as positive (MUM2B, C8161, and EW7) or negative (MUM2C, C81-61, RD-ES, and SIM) for their capacity to mimic an EL phenotype. Importantly, the expression of endogenous *ADAMTS1* is increased significantly in cells that exhibit EL properties (EL+ cells; Supplementary Fig. S1; Fig. 3A). Additional genes that were analyzed included *laminin 5γ2* and *TFPI-2*, which have already been shown to be differentially expressed in EL+ cells (23). Protein levels of ADAMTS1 were also evaluated (Fig. 3B). Phorbol 12-myristate 13-acetate (PMA) treatment was used to upregulate endogenous ADAMTS1 (24). ADAMTS1 protein levels were detected in the conditioned medium of EL+ cell lines, whereas very low or no detectable levels were detected in the nonaggressive cells. To confirm the activity of ADAMTS1, COOH-terminal cleavage of TFPI-2 in those cell lines was analyzed; the results revealed that the cleavage of TFPI-2 did coincide with the endogenous expression of ADAMTS1 (Supplementary Fig. S2).

In addition, we analyzed the expression of *ADAMTS1* in EW7-derived xenografts, a known EL+ tumor type (23), to

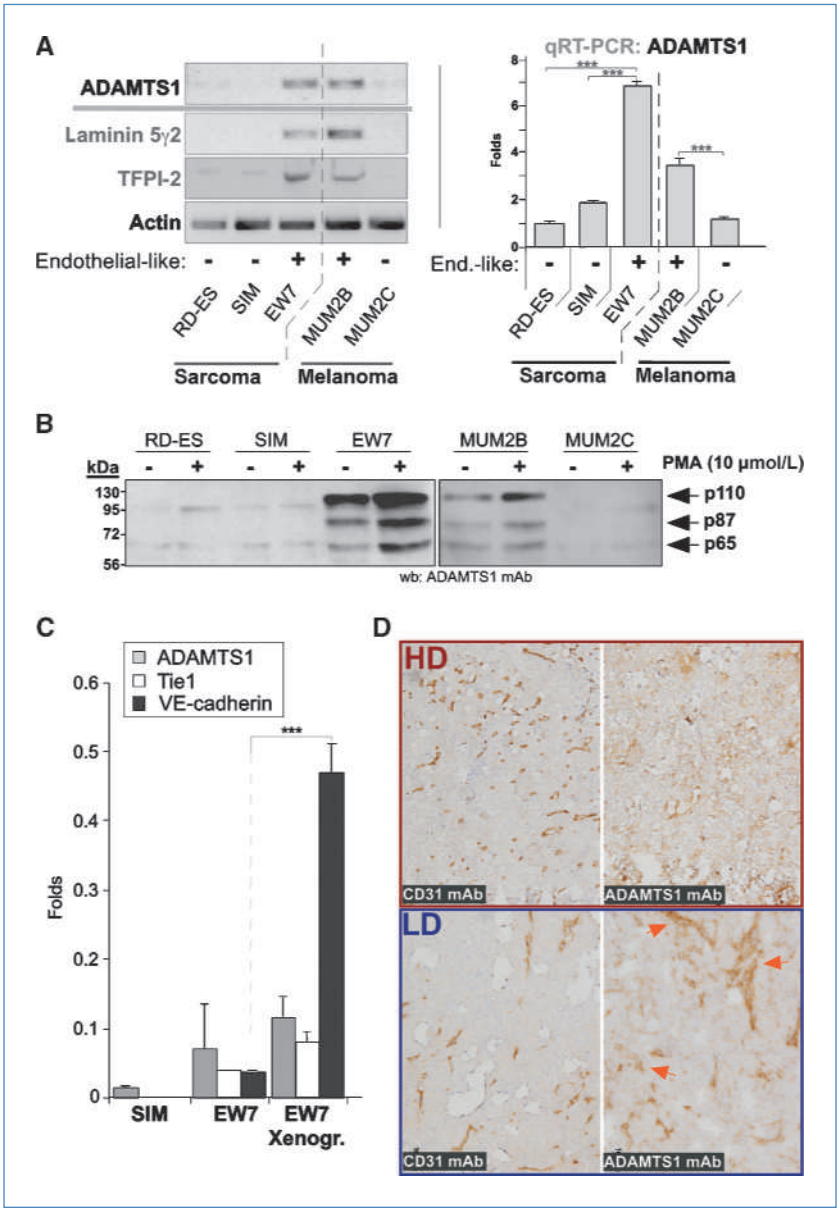

Figure 3. Presence of ADAMTS1 in melanoma and sarcoma cells. A, total RNA (0.5 μg) from sarcoma and melanoma cells was subjected to RT-PCR (left) and qRT-PCR (right) with specific oligos for the indicated genes. EL+ and EL– refers to the ability of these cells to form or not form capillary-like structures, respectively (***, $P < 0.001$, one-way ANOVA, Tukey's Multiple Comparison posttest). B, 48-h conditioned medium from the indicated cells was analyzed by Western blot. As indicated, cells were treated with PMA. Arrows, ADAMTS1 forms. C, total RNA (0.2 μg) from EL+ (EW7) and EL– (SIM) cells and EW7-derived xenograft samples was subjected to qRT-PCR with specific oligos for the indicated genes (***, $P < 0.001$, unpaired t test with Welch's correction). D, cryosections from EW7-derived xenografts were immunostained with antibodies for mouse CD31 and human ADAMTS1. Note the difference of ADAMTS1 pattern between areas with higher vascular density (HD; top) and low vessel density (LD; bottom). Arrows, locations where ADAMTS1 appears to be mainly stored.

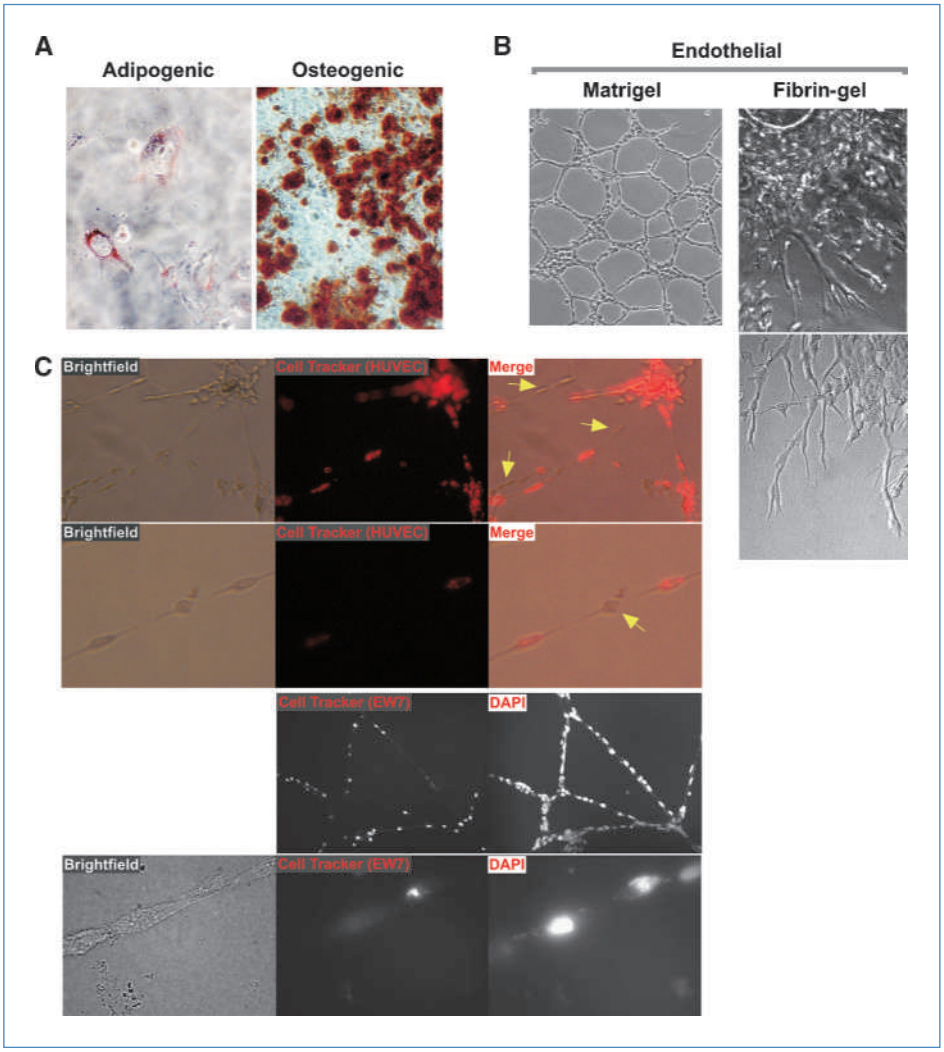

Figure 4. Tumor cell plasticity of EW7 sarcoma cells. A, EW7 cells were properly treated to differentiate into an adipogenic and osteogenic lineage. Fixed cells were stained with Oil Red O and Alizarin Red S to visualize the respective phenotypes. B, EL features of EW7 demonstrated by culture in Matrigel and fibrin gel matrices. For the fibrin gel model, two pictures are presented. C, HUVEC and EW7 cells were cocultured in Matrigel. Top, HUVEC were labeled with Cell Tracker. Merge panels show the coexistence of HUVEC and EW7 cells (pointed with yellow arrows) in capillary-like structures. Bottom, EW7 cells were labeled with Cell Tracker and all nuclei were counterstained with DAPI. All images were captured with ×5 and ×20 objectives.

determine the effect of a microenvironment on ADAMTS1. qRT-PCR was performed and compared with EW7 and SIM cell lines. In addition to *ADAMTS1,* endothelial-related markers *Tie1* and *VE-cadherin* were also evaluated as a measure of the progression of this tumor plasticity phenomenon. These analyses confirmed the presence of *ADAMTS1* in xenografts at comparable levels with its basal expression in cell culture (Fig. 3C). Finally, the presence of ADAMTS1 in tumor sections was evaluated by immunohistochemistry. Given the extracellular features of ADAMTS1, its localization *in situ* does not display well-defined patterns. A detailed study of tumor sections revealed distinct areas with various degrees of ADAMTS1 expression. Although those areas with high vessel density, determined by CD31 staining, presented a homogeneous positive signal for ADAMTS1 (Fig. 3D, top), the analysis of zones with a decreased density of CD31+ vessels, which is reminiscent of the reported EL+ events (23), revealed a more restricted pattern of ADAMTS1 staining. This is probably associated with extracellular reservoirs (pointed by arrows in Fig. 3D, bottom).

These results clearly indicated a high intratumor variability, which makes it difficult to track the expression of ADAMTS1 in human tumors. However, review of various public microarray analyses of human sarcomas allowed us to assess the role of protease ADAMTS1 (Supplementary Fig. S3).

Plasticity of sarcoma tumor cells

EW7 cells have a potential mesenchymal origin. This potential was shown by its ability to differentiate into an adipogenic and osteogenic lineage when maintained under proper conditions (Fig. 4A). The ability of these cells to acquire an EL phenotype was assessed through a series of Matrigel experiments (Fig. 4B). In addition, fibrin-based three-dimensional models were used to study the formation of endothelial-derived tubules (20). Importantly, formation of multicellular tubular structures by EW7 cells was observed in this assay (Fig. 4B).

To further prove the capacity of EW7 cells to share common properties with endothelial cells, EW7 cells were

cocultured with HUVECs in Matrigel. One of the cell types was stained with a fluorescent cell tracker to distinguish between the two cell types. Close analysis of the resulting capillary-like structures (Fig. 4C) confirmed the ability of EW7 cells to mimic the endothelial phenotype, which is characterized by aligning themselves, even individual cells (pointed with yellow arrows in Fig. 4C), in structures mainly formed by endothelial cells.

Impairment of capillary-like formation by the inhibition of ADAMTS1 and the use of specific metalloproteinase inhibitors

We have shown that overexpression of ADAMTS1 enhanced an EL phenotype in HT1080 fibrosarcoma cells. The next step was to investigate whether downregulation of this protease have an inhibitory effect on the endothelial properties of these cells. Therefore, we inhibited ADAMTS1 expression in EW7 cells by shRNA technology (Fig. 5A) and then evaluated the effect of its absence on the formation of capillary-like structures. At low cellular density (Fig. 5B), a clear delay over time and impairment of formation of structures were observed in cells with inhibited expression of ADAMTS1. However, cultures at high density required a deeper evaluation. Although all cells were apparently capable of forming capillary-like structures, knockdown ADAMTS1 cells displayed a loose appearance at brightfield capture, which was reminiscent of an ameboid-like conformation with no robust cell-cell contacts (Fig. 5C). To better visualize the impaired cell-cell contacts, the distribution of actin stress fibers was evaluated by phalloidin staining. In knockdown cells, actin fibers were accumulated at the border, more obvious at higher magnifications; in contrast, control cells displayed a more dispersed actin distribution (Fig. 5C). Knockdown ADAMTS1 cells appeared detached among themselves and the capillary-like structures that they formed were more fragile and unstable. No alterations were detected for VE-cadherin and laminin 5γ2 proteins (Supplementary Fig. S4).

We extended this characterization by the treatment of control cultures in Matrigel with specific protease inhibitors. ADAMTS1 is specifically inhibited by TIMP3 but not by TIMP1 (19). No obvious differences were observed at 4 hours of treatment; however, a 24-hour exposure to TIMP3 induced a clear effect (Fig. 5D). The formation of capillary-like structures was delayed and disrupted.

Finally, we investigated the potential regulation of the EL properties by the protease ADAMTS1 in the fibrin-based tubular assay (as showed in Fig. 4B). Comparative experiments with ADAMTS1-knockdown cells were performed. These experiments were done with low concentrations of serum (1%) to avoid the main proliferative response of these tumor cells, which would mask any differentiation-like process. Primary sprouts were evaluated at 24 hours; its formation was clearly inhibited in ADAMTS1-knockdown cells, as observed under the microscope (Fig. 6A). Quantification of the number of sprouts per bead (Fig. 6B) confirms a strong difference between control and inhibited cells.

Discussion

The current concept of tumor neovascularization is far from the classic view that explained such process solely by the growth of new vessels from preexisting ones (1, 24). In our attempt to contribute to the understanding of the mechanisms of action of ADAMTS1 during tumor progression, we obtained strong evidence that supports its participation in events of tumor plasticity that lead to alternative mechanisms of vascularization.

In the context of a fibrosarcoma model, we observed that although tumor growth was clearly increased in the presence of ADAMTS1, a close evaluation of vascularization revealed the presence of angiogenesis-independent networks. Although the participation of ADAMTS1 during tumor progression seemed controversial in literature, it is certainly striking that our tumor model displayed both a protumorigenic effect and an antiangiogenic response, as revealed by the decreased vascular density in those same tumors.

The analysis of the angiogenesis-independent networks showed similar characteristics to those previously identified in distinct tumor types. In addition to the enrichment with extracellular matrix components, we observed a clear upregulation of key proteins such as laminin 5γ2 and VE-cadherin, which is accompanied by a gene signature reminiscent of an endothelial nature. These characteristics were already associated with events of VM in melanoma (2). Surprisingly, our particular genetic characterization of HT1080 fibrosarcoma cells revealed the endogenous presence of endothelial-related genes. As far as we know, this EL phenotype of HT1080 cells has not been studied or reported. However, a plastic behavior of these cells has been described in a proteolytic-dependent manner (25, 26). Our work suggests that ADAMTS1 activity drives HT1080 plasticity to a definitive EL lineage.

After the evaluation of our xenografts and the initial characterization of ADAMTS1 on melanoma and Ewing sarcoma cells, we believed that we were facing an example of VM and tumor plasticity. The ability of tumor cells to differentiate into a specific cellular lineage, EL in our case, recapitulates many of the mechanisms that a normal stem cell undergoes to cause an endothelial cell and, by extension, a vascular structure. According to the nature of ADAMTS1, we can assume that its proteolytic-derived microenvironment modifications represent relevant clues to modulate phenotypic properties of tumor cells. ADAMTS1 exemplifies the capacity of extracellular matrix proteases to alter physical matrix properties; however, more studies are needed to further address this matter. Thus, it is important to identify the substrates of ADAMTS1 in a particular setting. Here, we showed the required coexpression of TFPI-2, which has already been reported as important for VM progression (27), and of the glycoprotein nidogen-1, a basic component of the vascular basement membrane, and identified as promoter of human embryonic stem cells assembly (28).

Although our initial results could be oriented to both melanoma and sarcoma tumor models, we decided to focus in sarcoma whose mesenchymal origin has provoked a relevant

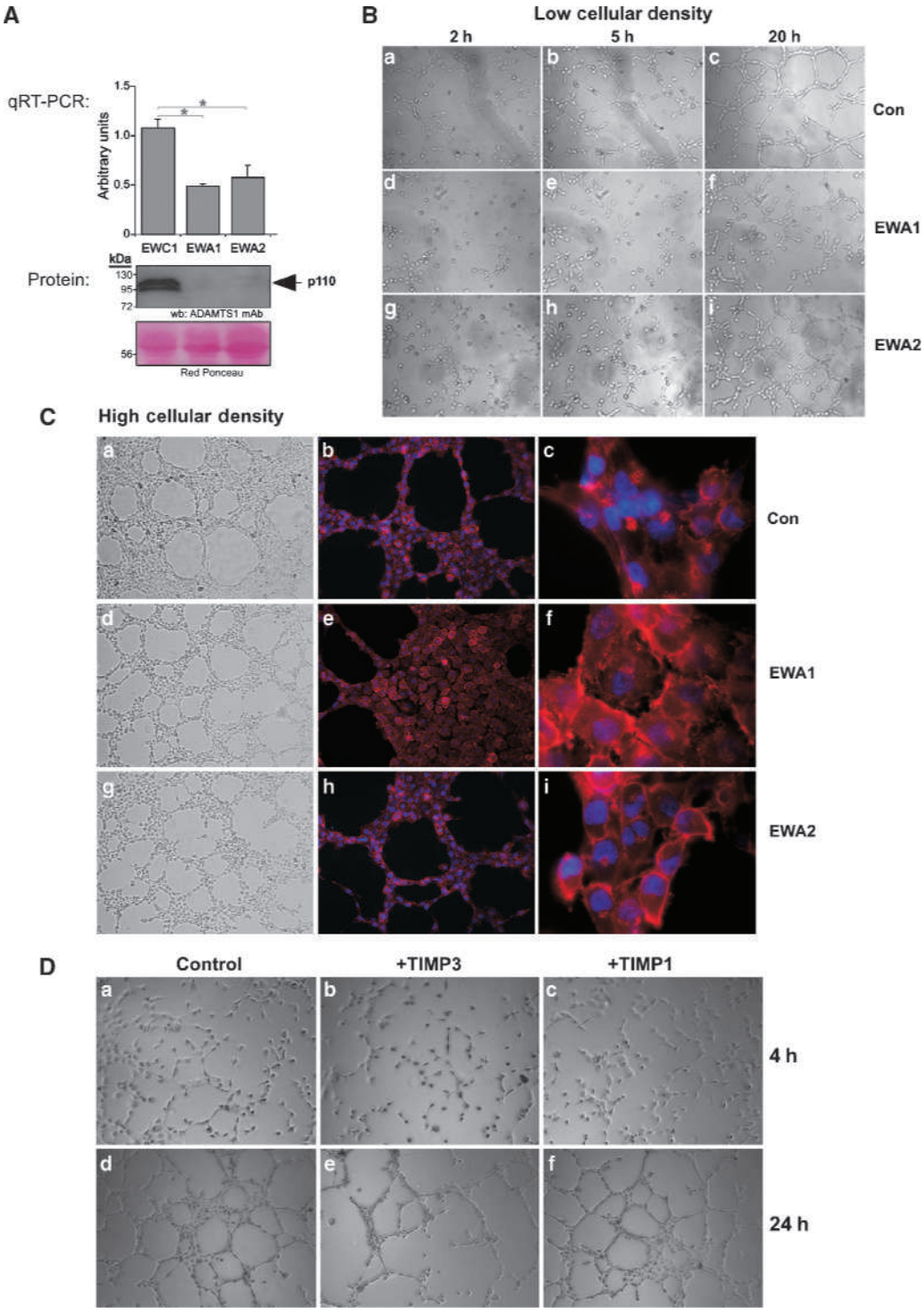

Figure 5. Impairment of capillary-like formation by the inhibition of ADAMTS1 and by specific metalloproteinase inhibitors. A, qRT-PCR and Western blot analysis for ADAMTS1 in control (EWC1) and knockdown-ADAMTS1 (EWA1 and EWA2) EW7 cells (*, $P < 0.05$, one-way ANOVA, Tukey's Multiple Comparison posttest). B, control and knockdown cells were cultured in Matrigel at low density. Brightfield pictures were taken at indicated time points with a ×10 objective. C, control and knockdown cells were cultured in Matrigel at high density. Cells were stained with phalloidin and DAPI at 18 h. Brightfield images (a, d, and g) were taken at ×10 magnification. Fluorescent images showed phalloidin and DAPI staining at ×10 (b, e, and h) and ×100 (c, f, and i). D, Matrigel assay with EW7 wild-type cells using TIMP3 and TIMP1. Pictures were captured at 4 and 24 h. All images were taken at ×10 magnification.

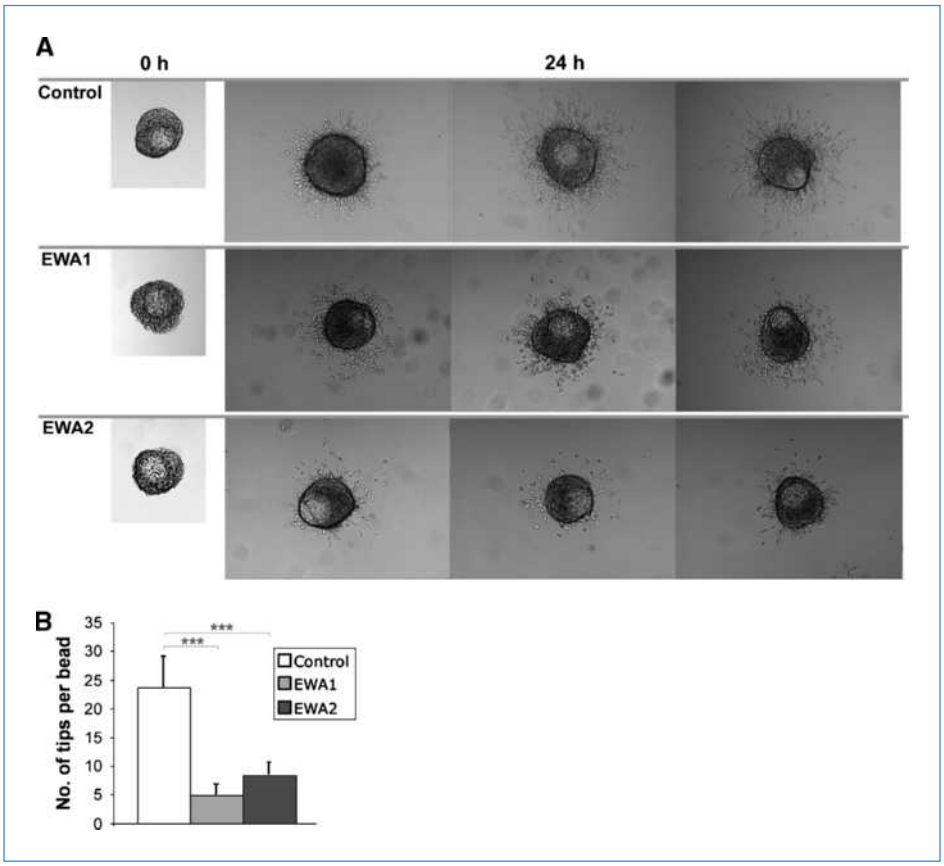

Figure 6. Inhibition of tube formation in the fibrin gel bead assay by downregulation of ADAMTS1. A, beads were coated with control and knockdown-ADAMTS1 EW7 cells. Coated beads were then embedded in fibrin gel and maintained for 24 h. Representative images were taken at 0 and 24 h. B, graphical representation of the quantification of tubular structures at 24 h since the embedding of cells in fibrin gels. For quantification, 12 random beads were pictured from six different experimental wells and cell sprouts were counted for each bead. (***, $P < 10^{-5}$, two-tail Student's *t* test).

debate in relation with CSC hypotheses (6–8, 29). In fact, the capacity of sarcoma cells to differentiate into mesenchymal-derived phenotypes has been shown in literature (30, 31). We were also able to reproduce this feature in our tumor model. An endothelial origin of Ewing tumors has also been proposed (4, 5) and the derivation of an endothelial lineage from mesenchymal progenitors has been shown (32, 33). In this context, it is mandatory to consider the aberrant nature of those tumor cells, whose plastic capabilities are under discussion. For example, van der Shaft and colleagues (23) suggested a hypoxic environment as a leading force that enhances the presence of alternative circulatory networks in Ewing sarcomas. Importantly, ADAMTS1 has been found to be regulated by hypoxia in endothelial cells (34). The convergence of embryonic and tumorigenic pathways has also been highlighted to determine this phenotypic plasticity (11). As for ADAMTS1, its contribution during embryonic development has been reported for myocardial morphogenesis (35) and its genetic deletion results in morphologic defects in various tissues (36). Although this role has not been extensively studied, our current results encourage new approaches to obtain a better perspective of ADAMTS1 activity during morphogenesis and cellular differentiation.

Here, we achieved the characterization of EL properties of EW7 tumor cells in Matrigel assays; moreover, we added unique information as the coculture approach with nontumorigenic endothelial cells. The evaluation of these assays confirmed the capacity of sarcoma cells to interact directly with endothelial cells and mimic their properties by alignment and formation of capillary-like structures in an apparently arbitrary pattern. These results supported the existence of bona fide functional interactions among endothelial and tumor cells in an *in vivo* context, as previously reported for human melanoma cells in a mouse model of ischemic limbs (37), and it also suggest that the VM phenomenon could consist of hybrid tumor-endothelial structures, with relevant consequences for the best understanding of its functionality (38).

In addition, we investigated the EL capabilities of Ewing tumor cells in the three-dimensional fibrin gel method that has been widely established to study the multistage formation of endothelial tubular structures (20). As noted in the main text, we did not obtain the same degree of success as for endothelial cells. However, it is important to notice that EW7-derived EL structures did not require the addition of fibroblast and/or additional growth factors, suggesting their autonomy, at least during initial stages of tube formation.

More important were our findings that both Matrigel and fibrin gel functional procedures were compromised by the

inhibition of ADAMTS1, as shown by shRNA technology and by treatment with specific protease inhibitors.

The contribution of extracellular proteases during tumor progression has been extensively evaluated. However, the complexity of their actions became evident after the failure of various clinical trials with protease inhibitors. In fact, the characterization of the substrates for every protease is of high significance in the field (39) and, by extension, the design of more specific inhibitors (40).

In conclusion, the dynamism of tumor microenvironment is crucial for the behavior of tumor cells, providing cues for proliferation, migration, and, as supported by this manuscript, differentiation of aberrant cells. Our findings also suggest the existence of functional CSCs, with major consequences for tumor progression contributing to an alternative mechanism of neovascularization, a phenomenon that requires a thoughtful characterization to help improve current therapies.

Disclosure of Potential Conflicts of Interest

No potential conflicts of interest were disclosed.

Acknowledgments

We thank Dr. J.A. Recio (Institut de Recerca Vall d'Hebron, Barcelona, Spain) for providing the lentiviral-related tools, Dr. M.L. Iruela-Arispe (University of California, Los Angeles, CA) for the ADAMTS1 antibodies, and Dr. Shelley N. Thai for the English editing.

Grant Support

Ministerio de Ciencia e Innovación-Spain (SAF2006-04019), Instituto de Salud Carlos III (EMER07/055), and Fundaciò La Marató de TV3 (052510).

The costs of publication of this article were defrayed in part by the payment of page charges. This article must therefore be hereby marked *advertisement* in accordance with 18 U.S.C. Section 1734 solely to indicate this fact.

Received 11/16/2009; revised 03/19/2010; accepted 03/24/2010; published OnlineFirst 05/18/2010.

References

1. Dome B, Hendrix MJ, Paku S, et al. Alternative vascularization mechanisms in cancer: pathology and therapeutic implications. Am J Pathol 2007;170:1–15.
2. Hendrix MJ, Seftor EA, Hess AR, Seftor RE. Vasculogenic mimicry and tumour-cell plasticity: lessons from melanoma. Nat Rev Cancer 2003;3:411–21.
3. Maniotis AJ, Folberg R, Hess A, et al. Vascular channel formation by human melanoma cells *in vivo* and *in vitro*: vasculogenic mimicry. Am J Pathol 1999;155:739–52.
4. Ewing J. Diffuse endothelioma of bone. Proc N Y Pathol Soc 1921; 21:17–24.
5. Staege MS, Hutter C, Neumann I, et al. DNA microarrays reveal relationship of Ewing family tumors to both endothelial and fetal neural crest-derived cells and define novel targets. Cancer Res 2004;64: 8213–21.
6. Charytonowicz E, Cordon-Cardo C, Matushansky I, Ziman M. Alveolar rhabdomyosarcoma: Is the cell of origin a mesenchymal stem cell? Cancer Lett 2009;279:126–36.
7. Matushansky I, Hernando E, Socci ND, et al. Derivation of sarcomas from mesenchymal stem cells via inactivation of the Wnt pathway. J Clin Invest 2007;117:3248–57.
8. Tirode F, Laud-Duval K, Prieur A, et al. Mesenchymal stem cell features of Ewing tumors. Cancer Cell 2007;11:421–9.
9. Engler AJ, Sen S, Sweeney HL, Discher DE. Matrix elasticity directs stem cell lineage specification. Cell 2006;126:677–89.
10. Butcher DT, Alliston T, Weaver VM. A tense situation: forcing tumour progression. Nat Rev Cancer 2009;9:108–22.
11. Hendrix MJ, Seftor EA, Seftor RE, et al. Reprogramming metastatic tumour cells with embryonic microenvironments. Nat Rev Cancer 2007;7:246–55.
12. Jones DL, Wagers AJ. No place like home: anatomy and function of the stem cell niche. Nat Rev Mol Cell Biol 2008;9:11–21.
13. Apte SS. A disintegrin-like and metalloprotease (reprolysin-type) with thrombospondin type 1 motif (ADAMTS) superfamily: functions and mechanisms. J Biol Chem 2009;284:31493–7.
14. Luque A, Carpizo DR, Iruela-Arispe ML. ADAMTS1/METH1 inhibits endothelial cell proliferation by direct binding and sequestration of VEGF165. J Biol Chem 2003;278:23656–65.
15. Vazquez F, Hastings G, Ortega MA, et al. METH-1, a human ortholog of ADAMTS-1, and METH-2 are members of a new family of proteins with angio-inhibitory activity. J Biol Chem 1999;274:23349–57.
16. Rocks N, Paulissen G, Quesada-Calvo F, et al. ADAMTS-1 metalloproteinase promotes tumor development through the induction of a stromal reaction *in vivo*. Cancer Res 2008;68:9541–50.
17. Liu YJ, Xu Y, Yu Q. Full-length ADAMTS-1 and the ADAMTS-1 fragments display pro- and antimetastatic activity, respectively. Oncogene 2006;25:2452–67.
18. Lu X, Wang Q, Hu G, et al. ADAMTS1 and MMP1 proteolytically engage EGF-like ligands in an osteolytic signaling cascade for bone metastasis. Genes Dev 2009;23:1882–94.
19. Rodriguez-Manzaneque JC, Westling J, Thai SN, et al. ADAMTS1 cleaves aggrecan at multiple sites and is differentially inhibited by metalloproteinase inhibitors. Biochem Biophys Res Commun 2002; 293:501–8.
20. Nakatsu MN, Hughes CC. An optimized three-dimensional *in vitro* model for the analysis of angiogenesis. Methods Enzymol 2008; 443:65–82.
21. Matar P, Rojo F, Cassia R, et al. Combined epidermal growth factor receptor targeting with the tyrosine kinase inhibitor gefitinib (ZD1839) and the monoclonal antibody cetuximab (IMC-C225): superiority over single-agent receptor targeting. Clin Cancer Res 2004;10: 6487–501.
22. Sood AK, Seftor EA, Fletcher MS, et al. Molecular determinants of ovarian cancer plasticity. Am J Pathol 2001;158:1279–88.
23. van der Schaft DW, Hillen F, Pauwels P, et al. Tumor cell plasticity in Ewing sarcoma, an alternative circulatory system stimulated by hypoxia. Cancer Res 2005;65:11520–8.
24. Auguste P, Lemiere S, Larrieu-Lahargue F, Bikfalvi A. Molecular mechanisms of tumor vascularization. Crit Rev Oncol Hematol 2005;54:53–61.
25. Wolf K, Mazo I, Leung H, et al. Compensation mechanism in tumor cell migration: mesenchymal-amoeboid transition after blocking of pericellular proteolysis. J Cell Biol 2003;160:267–77.
26. Wolf K, Wu YI, Liu Y, et al. Multi-step pericellular proteolysis controls the transition from individual to collective cancer cell invasion. Nat Cell Biol 2007;9:893–904.
27. Ruf W, Seftor EA, Petrovan RJ, et al. Differential role of tissue factor pathway inhibitors 1 and 2 in melanoma vasculogenic mimicry. Cancer Res 2003;63:5381–9.
28. Evseenko D, Schenke-Layland K, Dravid G, et al. Identification of the critical extracellular matrix proteins that promote human embryonic stem cell assembly. Stem Cells Dev 2009;18:919–28.
29. Riggi N, Cironi L, Provero P, et al. Expression of the FUS-CHOP fusion protein in primary mesenchymal progenitor cells gives rise to a model of myxoid liposarcoma. Cancer Res 2006;66:7016–23.
30. Riggi N, Suva ML, Suva D, et al. EWS-FLI-1 expression triggers a Ewing's sarcoma initiation program in primary human mesenchymal stem cells. Cancer Res 2008;68:2176–85.
31. Suva ML, Riggi N, Stehle JC, et al. Identification of cancer stem cells in Ewing's sarcoma. Cancer Res 2009;69:1776–81.

32. Liu JW, Dunoyer-Geindre S, Serre-Beinier V, et al. Characterization of endothelial-like cells derived from human mesenchymal stem cells. J Thromb Haemost 2007;5:826–34.
33. Oswald J, Boxberger S, Jorgensen B, et al. Mesenchymal stem cells can be differentiated into endothelial cells *in vitro*. Stem Cells 2004; 22:377–84.
34. Hatipoglu OF, Hirohata S, Cilek MZ, et al. ADAMTS1 is a unique hypoxic early response gene expressed by endothelial cells. J Biol Chem 2009;284:16325–33.
35. Stankunas K, Hang CT, Tsun ZY, et al. Endocardial Brg1 represses ADAMTS1 to maintain the microenvironment for myocardial morphogenesis. Dev Cell 2008;14:298–311.
36. Shindo T, Kurihara H, Kuno K, et al. ADAMTS-1: a metalloproteinase-disintegrin essential for normal growth, fertility, and organ morphology and function. J Clin Invest 2000;105:1345–52.
37. Hendrix MJ, Seftor RE, Seftor EA, et al. Transendothelial function of human metastatic melanoma cells: role of the microenvironment in cell-fate determination. Cancer Res 2002;62:665–8.
38. McDonald DM, Munn L, Jain RK. Vasculogenic mimicry: how convincing, how novel, and how significant? Am J Pathol 2000;156: 383–8.
39. Lopez-Otin C, Overall CM. Protease degradomics: a new challenge for proteomics. Nat Rev Mol Cell Biol 2002;3:509–19.
40. Overall CM, Lopez-Otin C. Strategies for MMP inhibition in cancer: innovations for the post-trial era. Nat Rev Cancer 2002;2: 657–72.